IDENTIFICATION OF SILICON WAFERS DEFECTS BASED ON METHOD OF DISCRETE SOURCES

Yu. Eremin and N. Orlov

Applied Math & Computer Science Faculty of the Moscow State University
Vorobyov Hills, Moscow 117899, Russia
eremin@cs.msu.su

Abstract

The Method of Discrete Sources (MDS) was applied to construct complete mathematical models of light scattering from various kinds of defects on silicon wafers. In this paper the wafer defects are contaminating particles, surface defects (pits), and/or subsurface defects (bulks). A heuristic approach was suggested as a tool for a qualitative analysis of scattering from wafer defects. Numerical results demonstrate the advantage of the proposed technique.

1. INTRODUCTION

The foregoing miniaturization of microchips and increasing of numbers of elements at the same area of surface come to be a real factor of a technical progress in the last decades. Being a first-step chain for the chip manufacturing silicon wafers demand an extra care of their purity, which is determined by certain defects of real wafers: contaminating micro-particles, pits and subsurface bulks, some other defects. The purity monitoring is being carried out through special devices, namely surface scanners, where special collectors for analysis of scattered from wafer defect light are in use. As a rule, these devices use a laser source of light. Scanners of such a kind are developed for determination of wafer defect characterization: the number, type and size of contaminants, and their locations as well. The wafer manufacturers at the present tend to monitoring defects as small as 0.06 μm.

One of important problems to be solved is a determination of the contaminant size and material. The other one, very new, is the identification of defects of various kinds. In particular, how to distinguish a contaminating particle from a pit or a subsurface defect. The last problem seems to be even more important than identification of the material of a contaminating particle, because at the present any wafer defects are treated by scanners as particles. In order to remove those defects the chemical cleaning of surface is carried out. As a result, the number of particle decrease, yet pits only grow instead, or

subsurface defects transform to new pits. When sounding repeatedly scanner again figures out a pit as a particle but just having a bigger size. So that, the further "cleaning" of a surface can have a complete damage of wafer as a result.

In this paper a new approach is developed allowing to analyze a scattering of TM or TE polarized plane wave from a penetrable particle, subsurface defect or pit on the surface of silicon wafer. On the base of the Method of Discrete Sources (MDS) a program is developed enabling to carry out a numerical analysis of defects of different kinds. Based on results of mathematical simulation and numerical experiments characteristic features of defects are established, that helps their identification.

2. MODEL I: PENETRABLE PARTICLE ON SUBSTRATE

Let us start from the Boundary Value Scattering Problem (BVSP). Let $\{\mathbf{E}^0, \mathbf{H}^0\}$ to be a field of time-harmonic plane electromagnetic wave of linear polarization. The plane wave is assumed to propagate in direction with an angle γ of a normal to the plane Ξ, an air-substrate interface. Denote two half-spaces with D_0 (air) and D_1 (substrate), see Fig. 1.

Let an axi-symmetrical scatterer D_i having a smooth surface ∂D to be located at the interface in such a way that its symmetry axis to be parallel to an external normal of the interface Ξ. Then introduce into consideration a Cartesian coordinate system, choosing its origin at the touching point of scatterer D_i, and take Oz axis to be directed into D_0, as it is shown in the Fig. 1. Then the BVSP can be stated as follow:

$$\nabla \times \mathbf{H}_t = ik\varepsilon_t \mathbf{E}_t; \quad \nabla \times \mathbf{E}_t = -ik\mu_t \mathbf{H}_t \quad \text{in } D_t, \quad t = 0,1,i, \tag{1.1a}$$

$$\begin{aligned} &\mathbf{n}_p \times \left(\mathbf{E}_i(p) - \mathbf{E}_0^s(p)\right) = \mathbf{n}_p \times \mathbf{E}^0(p), \\ &\mathbf{n}_p \times \left(\mathbf{H}_i(p) - \mathbf{H}_0^s(p)\right) = \mathbf{n}_p \times \mathbf{H}^0(p), \end{aligned} \quad p \in \partial D, \tag{1.1b}$$

$$\begin{aligned} &\mathbf{e}_z \times \left(\mathbf{E}_0(p) - \mathbf{E}_1(p)\right) = 0, \\ &\mathbf{e}_z \times \left(\mathbf{H}_0(p) - \mathbf{H}_1(p)\right) = 0, \end{aligned} \quad p \in \Xi, \tag{1.1c}$$

radiation/attenuation conditions at infinity ($z \neq 0$). (1.1d)

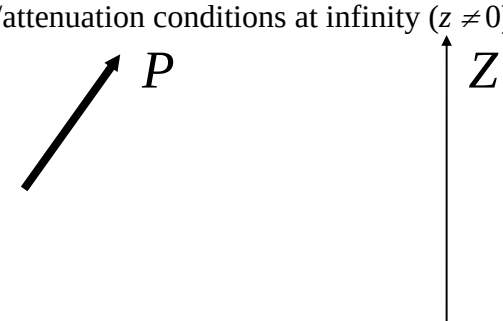

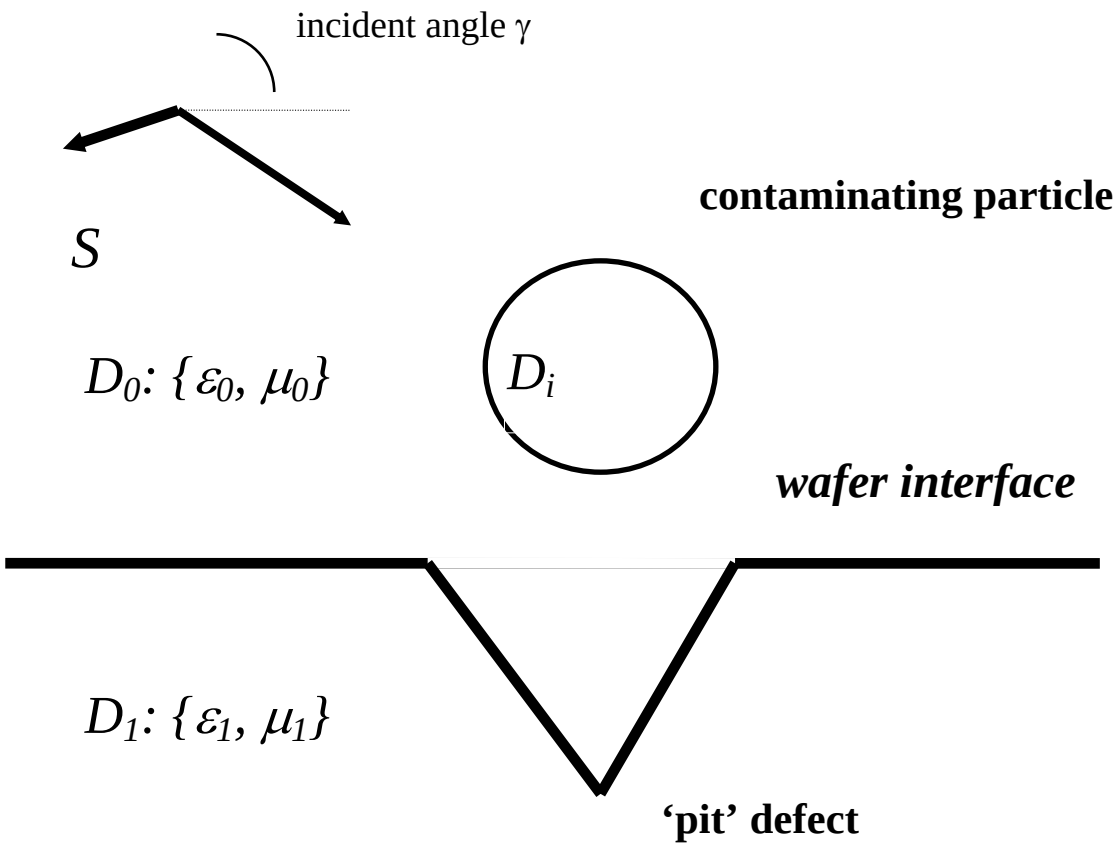

Figure 1. Geometry of the problem

Here $k = \omega / c$, $\left\{\mathbf{E}_0^s, \mathbf{H}_0^s\right\}$ is a scattered field in D_0, and medium parameters fit the condition $\operatorname{Im} \varepsilon_t, \mu_t \le 0$, the time dependence is chosen as $\exp\left\{i\omega t\right\}$.

Let us construct an approximate solution to BVSP (1) on the base of MDS [1]. For this goal let us represent the external excitation as a total of incident and reflected plane waves at the upper half-space (D_0) and refracted wave at the lower half-space (D_1). Thus, at the upper half-space (D_0) it is sufficient to construct a representation for a scattered field only. The idea of MDS is to construct a scattered field as a finite linear combination of multipoles' fields, so this combination would fit the Maxwell equations at fields D_0, D_1, D_i; at infinity: the radiation conditions in D_0, and the attenuation conditions in D_1, (the silicon is supposed to have an attenuation); and also the

transmission conditions for tangential components of fields at the interface (that is an essential point). Under these conditions the solution of BVSP (1) is being reduced to an approximation of the external field at the particle surface via multipoles' fields. So that the determination of unknown amplitudes of discrete sources is being carried out from transmission conditions at the particle surface ∂D. The advantage of this approach is the opportunity to estimate the defect of the solution obtained through calculation of the residual of boundary values at ∂D. Let us construct the representation of approximate solution in such a way to take into consideration auxiliary the axial symmetry of an obstacle and polarization of inclining plane wave. A similar approach has been used by the authors in some previous works for calculation of scattering from particle in free space [4]. Let us put the multipole sources of electric (*e*) and magnetic (*m*) kinds to the base of external field representation in such a way that the Hertz vectors for these poles have a form

$$\mathbf{A}_{mx}^{e,h} = \mathbf{e}_x\, g_m^{e,h} + \mathbf{e}_z(\mathbf{e}_x, \nabla)\, f_m, \qquad \mathbf{A}_{my}^{e,h} = \mathbf{e}_y\, g_m^{e,h} + \mathbf{e}_z(\mathbf{e}_y, \nabla)\, f_m,$$

with $\mathbf{e}_x, \mathbf{e}_y, \mathbf{e}_z$ being Cartesian orts. We remind, the structure of such a form is determined by a half-space [3] presence and can be explained in the terms of Green tensor structure ($\dim \overleftrightarrow{\mathbf{G}} = 3 \times 3$). The elements $g_m^{e,h}$ and $f_m^{e,h}$ are produced by elements $G_{11}^{e,h}$, $G_{22}^{e,h}$ and $G_{31}^{e,h}$, $G_{32}^{e,h}$ of the Green tensor $\overleftrightarrow{\mathbf{G}}^{e,h}(M, P)$ [3]. Then,

$$g_m^{e,h}(q, w_n) = Y_m^0(q, w_n) - Y_m^0(q, -w_n) + \int_0^\infty J_m(\lambda\rho)\, \kappa^{e,h} \exp\{-\eta_0(z + w_n)\}\, \lambda^{1+m} d\lambda\,, \tag{1.2a}$$

$$f_m(q, w_n) = \int_0^\infty J_m(\lambda\rho)\, \zeta \exp\{-\eta_0(z + w_n)\}\, \lambda^{1+m} d\lambda,$$

$$Y_{nm}^0(q) = Y_m^0(q, w_n) = \frac{k_0}{i} h_m^{(2)}(k_0 R_{qw_n}) \times (k_0\, \rho / R_{qw_n})^m$$

$$R_{qw_n}^2 = \rho^2 + (z - w_n)^2, \qquad q = (\rho, z),$$

where $J_m(.)$ is the Bessel cylindrical function, and $h_m^{(2)}(.)$ is the Hankel spherical function; the point q lies at the half-plane ϕ = const, and poles are located at the Oz symmetry axis: $w_n \in Oz$. Spectral functions $\kappa^{e,h}$ and ζ are

$$\begin{aligned}
&\kappa^e = 2\mu_1/(\mu_1\eta_0 + \mu_0\eta_1), \quad \kappa^h = 2\varepsilon_1/(\varepsilon_1\eta_0 + \varepsilon_0\eta_1),\\
&\zeta = 2(\mu_1\varepsilon_1 - \mu_0\varepsilon_0)/\{(\varepsilon_1\eta_0 + \varepsilon_0\eta_1)(\mu_1\eta_0 + \mu_0\eta_1)\},\\
&\eta_{0,1}^2 = \lambda^2 - k_{0,1}^2, \quad k_{0,1}^2 = k^2\varepsilon_{0,1}\mu_{0,1}
\end{aligned} \tag{1.2b}$$

Since the particle is located in the upper half-space D_0, the field representation inside the substrate D_1 is not effected. Nevertheless, this representation will be considered later, assuming that it can be deduced in a similar way.

The representation for fields inside defect is based on the poles having singularities at the infinity [3]

$$\begin{aligned}
&\mathbf{A}_{mx}^i = g_m^i(q, w_n)\mathbf{e}_x, \qquad \mathbf{A}_{my}^i = g_m^i(q, w_n)\mathbf{e}_y,\\
&g_m^i(q, w) = j_m(k_i R_{qw}) \times (k_i\ \rho / R_{qw})^m,
\end{aligned}$$

where $j_m(.)$ is the spherical Bessel function. Now formally we must just construct representations of EM fields inside and outside particle. This can be done taking into account not only the axial symmetry of the obstacle, but also the exciting field polarization [4].

Now consider the field of TM-polarized (the electric vector lies at the incident plane) plane EM wave, propagating under an angle γ to Oz axis. Then a total field of plane wave at the upper half-space can be written as follows

$$\begin{aligned}
&\mathbf{E}^0 = \mathbf{e}_x \cos\gamma\ (\chi_1 - R_P\ \chi_2) + \mathbf{e}_z \sin\gamma\ (\chi_1 + R_P\ \chi_2),\\
&\mathbf{H}^0 = -\mathbf{e}_y \cos\gamma\ (\chi_1 + R_P\ \chi_2),\\
&\chi_1 = \exp\{-ik_e(x\sin\gamma - z\cos\gamma)\},\\
&\chi_2 = \exp\{-ik_e(x\sin\gamma + z\cos\gamma)\},
\end{aligned} \tag{1.3a}$$

where the Fresnel coefficient in TM-case is [5]

$$R_P = \frac{\varepsilon_1 \cos\gamma - (\varepsilon_1 - \sin^2\gamma)^{1/2}}{\varepsilon_1 \cos\gamma + (\varepsilon_1 - \sin^2\gamma)^{1/2}} \ . \tag{1.3b}$$

In order to take into consideration the polarization of an external field, let's introduce the following combinations of vector potentials:

$$\begin{cases} \mathbf{A}^e_{\upsilon 0} = \mathbf{A}^e_{mx} \cos m\phi - \mathbf{A}^e_{my} \sin m\phi, \\ \mathbf{A}^h_{\upsilon 0} = \mathbf{A}^h_{mx} \sin m\phi + \mathbf{A}^h_{my} \cos m\phi, \end{cases} \quad \begin{cases} \mathbf{A}^e_{\upsilon i} = \mathbf{A}^i_{mx} \cos m\phi - \mathbf{A}^i_{my} \sin m\phi, \\ \mathbf{A}^h_{\upsilon i} = \mathbf{A}^i_{mx} \sin m\phi + \mathbf{A}^i_{my} \cos m\phi, \end{cases} \tag{1.4.a}$$

$\upsilon = \{m, n\}$ is a multiple index: $0 \le m \le M, \quad 1 \le n \le N$, here M is a maximal number of harmonics, and N is the multipoles number, being the same for the all range of m. Let's denote υ_0, Y: $\upsilon_0 = \{0,1\}, \quad Y = \{M, N\}$ are minimal and maximal values of the multiple index. Besides that take into consideration vector potentials to describe dipole sources

$$\mathbf{A}^e_{n0} = \sigma^e(q, w_n)\mathbf{e}_z, \quad \mathbf{A}^e_{ni} = g^i_0(q, w_n)\mathbf{e}_z, \quad \sigma^e = g^h_0(q, w_n) \tag{1.4b}$$

For convenience let's introduce the shorthand notation of fields, which will be used for constructing an approximate solution

$$\begin{pmatrix} \mathbf{E}^e_{\upsilon t} \\ \mathbf{H}^e_{\upsilon t} \end{pmatrix} = \begin{pmatrix} i/k\varepsilon_t\mu_t & \nabla\times\nabla\times \\ -1/\mu_t & \nabla\times \end{pmatrix} \mathbf{A}^e_{\upsilon t}, \quad \begin{pmatrix} \mathbf{E}^h_{\upsilon t} \\ \mathbf{H}^h_{\upsilon t} \end{pmatrix} = \begin{pmatrix} 1/\varepsilon_t & \nabla\times \\ i/k\varepsilon_t\mu_t & \nabla\times\nabla\times \end{pmatrix} \mathbf{A}^h_{\upsilon t} \ .$$

According to the notations introduced we construct the representation of BVSP (1) for TM-case in the form

$$\begin{pmatrix} \mathbf{E}^Y_t \\ \mathbf{H}^Y_t \end{pmatrix} = \sum_{\upsilon=\upsilon_0}^{Y} \left\{ p^t_\upsilon \begin{pmatrix} \mathbf{E}^e_{\upsilon t} \\ \mathbf{H}^e_{\upsilon t} \end{pmatrix} + q^t_\upsilon \begin{pmatrix} \mathbf{E}^h_{\upsilon t} \\ \mathbf{H}^h_{\upsilon t} \end{pmatrix} \right\} + \sum_{n=1}^{N} r^t_n \begin{pmatrix} \mathbf{E}^e_{nt} \\ \mathbf{H}^e_{nt} \end{pmatrix} . \tag{1.5}$$

As mentioned previously, the representation (1.5) satisfies all the conditions of BVSP (1.1) except transmission condition at the particle surface. By the analogy of the free space case [4] the potentials (1.4) are easily seen to be constructed in accordance with TM polarization of the external excitation (1.3).

In TE case (when $\mathbf{E}^0$ vector is orthogonal to the incident plane) the incident field is written as follows

$$\begin{aligned} \mathbf{E}^0 &= \mathbf{e}_y \cos\gamma\,(\chi_1 - R_S\,\chi_2), \\ \mathbf{H}^0 &= \mathbf{e}_x \cos\gamma\,(\chi_1 + R_S\,\chi_2) + \mathbf{e}_z \sin\gamma\,(\chi_1 - R_S\,\chi_2). \end{aligned} \tag{1.6a}$$

The Fresnel coefficient for TE-polarization has a form [5]

$$R_S = -\frac{\cos\gamma - (\varepsilon_1/\varepsilon_0 - \sin^2\gamma)^{1/2}}{\cos\gamma + (\varepsilon_1/\varepsilon_0 - \sin^2\gamma)^{1/2}}\ . \tag{1.6b}$$

In this case the approximate solution to BVSP (1.1) will has a form (1.5), yet instead of potentials (1.4a) we use following combinations

$$\begin{cases} \mathbf{A}^e_{\upsilon 0} = \mathbf{A}^e_{mx}\sin m\phi + \mathbf{A}^e_{my}\cos m\phi, \\ \mathbf{A}^h_{\upsilon 0} = \mathbf{A}^h_{mx}\cos m\phi - \mathbf{A}^h_{my}\sin m\phi, \end{cases} \quad \begin{cases} \mathbf{A}^e_{\upsilon i} = \mathbf{A}^i_{mx}\sin m\phi + \mathbf{A}^i_{my}\cos m\phi, \\ \mathbf{A}^h_{\upsilon i} = \mathbf{A}^i_{mx}\cos m\phi - \mathbf{A}^i_{my}\sin m\phi. \end{cases} \tag{1.7a}$$

Besides, the last term in the right-hand side (1.5), the dipole component, contains instead of a field $\{\mathbf{E}^e_{nt},\ \mathbf{H}^e_{nt}\}$ the field $\{\mathbf{E}^h_{nt},\ \mathbf{H}^h_{nt}\}$, produced by the vector potentials of the kind

$$\mathbf{A}^h_{n0} = \sigma^h(q, w_n)\mathbf{e}_z, \quad \mathbf{A}^h_{ni} = g^i_0(q, w_n)\mathbf{e}_z, \quad \sigma^h = g^e_0(q, w_n)\,. \tag{1.7b}$$

The dipole component in (1.7b) has such a form because in TE-case $\mathbf{H}^0$ vector lies at the incident plane.

So, the approximate solution to BVSP (1.1), where the vector multipole sources constructed in a special way are included, has a following properties:

1) fits the Maxwell equations inside a particle and in both half-spaces;

2) automatically satisfies the transmission condition for tangential components of fields at the interface Ξ;

3) satisfies the radiation/attenuation conditions at infinity.

Due to the completeness of the multipole system [3] and the orthogonality property of the multipole system for TM and TE polarizations at an arbitrary axi-symmetrical surface the following result take place.

Theorem 1. Let $\{\mathbf{E}^0,\ \mathbf{H}^0\}$: (1.3)/(1.6) then there exists Y and such coefficients $\{p_\upsilon, q_\upsilon\}_{\upsilon=\upsilon_0}^{\mathrm{Y}}$ that the field $\{\mathbf{E}^{\mathrm{Y}},\ \mathbf{H}^{\mathrm{Y}}\}$: (1.5), where the vector potentials (1.4)/(1.7) converge uniformly to the $\left\{\mathbf{E}_0^s, \mathbf{H}_0^s\right\}$ exact solution of BVSP (1.1) while $\mathrm{Y} \Rightarrow \infty$ at any closed compact outside the scatterer.

As noticed above, the approximate solution (1.5) satisfies all the conditions of BVSP (1.1) except transmission conditions at the particle surface. Let us introduce into consideration the amplitudes vector $\mathbf{p} := \left\{\mathrm{p}_\upsilon^{\mathrm{t}}, q_\upsilon^{\mathrm{t}}, r_n^{\mathrm{t}}\right\}_{\upsilon_0}^{\mathrm{Y}}$. As far as we try to approximate scattering characteristics in the far zone it is quite sufficient to provide a minimum of the field residual at the particle surface in $L_2(\partial D)$ norm [3].

The numerical algorithm for the determination of pole amplitudes seems to be more convenient as split into few steps. Because sources are located at *Oz* axis, the approximate solution (1.5) to BVSP (1.1) represents itself a finite linear combination of azimuth harmonics. So, at the first step tangential components of electric and magnetic fields of exciting plane wave are expanded into Fourier series on ϕ variable, using the following representation for plane wave

$$\exp\{-i\varpi\cos\phi\} = \sum_{m=0}^{\infty}(2-\delta_{0m})\,(-i)^m\,J_m(\varpi)\cos m\phi\ ,$$

where $\varpi = k_0\,\rho\sin\gamma$. As the representation (1.5) for the field $\{\mathbf{E}_t^{\mathrm{Y}},\ \mathbf{H}_t^{\mathrm{Y}}\}$ has a form of finite linear combination of Fourier harmonics with a dependence on the azimuth angle as $\sin m\phi$ and $\cos m\phi$ (t.i. a trigonometrical polynomial), then the determination of pole amplitudes is being deduced to the determination of the amplitude vector p for each azimuth harmonics (i.e. for a fixed harmonics number). As a result, the problem of surface approximation is being reduced to an approximation of field azimuth harmonics at the particle surface element $\Im$ [4].

For a solving of this task we use the collocation method, i.e. the matching of azimuth harmonics at the set of collocation points $\{\chi_\ell\}_{\ell=1}^{L} \subset \Im$ at the particle generatrix $\Im$. We should notice here, that both asymptotic evaluations [3] and numerical experience show the use of overdetermined systems enables to realize the most reliable numerical scheme for the amplitudes determination.

Each such system of linear algebraic equations (SLAE), corresponding to certain azimuth harmonics, is an overdetermined one of dimension $4L \times 4N$. For a harmonics not depending on ϕ we have a separate SLAE of size $2L \times 2N$ [4].

Remind, the different representations to an approximate solution, depending on the excitation polarization were proposed. However, the feature of the approach presented is a possibility to use the same matrix (for a fixed azimuth harmonics) either for TM or TE case. Thus, the determination of unknown pole amplitudes for TM and TE cases is being reduced to the duplex solving of SLAE having the same matrix but different right-hand sides.

In practice, the number L of collocation points is chosen from a usual approximational relation for sine-shaped functions: 8-10 points per each wavelength; while the number N of poles is chosen less than L. We usually take N from an heuristic relation $L > 1.5N$, that is quite sufficient for a reliable determination of pole amplitudes while $N \to \infty$. The maximal harmonics number M is chosen from the condition of good approximation of the plane wave by the finite piece of the Fourier series.

Note, the estimation of a quality of the exciting field at the particle surface allows us to establish a reliable monitoring of an approximate solution to BVSP (1.1) as aiming for faithful one. The residual calculation is important to being calculated at the whole particle surface, not only at the collocation points, with using as an external excitation the field of plane wave non expanded in Fourier series.

One of the basic scattering characteristics is the far field pattern, being determined as

$$\mathbf{E}(\mathbf{r}) \big/ \left|\mathbf{E}^0(\mathbf{r})\right| = \frac{\exp\{-ik_0 r\}}{r}\mathbf{F}(\theta,\phi) + O(1/r^2), \qquad r \to \infty .$$

Let's use an asymptotic approach [6] for a calculations of integrals of a kind

$$\int_0^\infty J_m(\lambda\rho)\ f(\lambda)\ \exp\{-\eta_0(z-w_n)\}\ \lambda^{1+m}d\lambda =$$

$$\psi_0\ ik_0\cos\theta\,(ik_0\sin\theta)^m G_n f(k_0\sin\theta) + o(1/r),\quad r\to\infty$$

where $\psi_0 = \exp\{-ik_0 r\}/r$, $G_n = \exp\{-ik_0 w_n\cos\theta\}$, $r^2 = \rho^2 + z^2$. Basing on this formula the asymptotics for Green tensor elements in the far zone can be obtained, and so the far field pattern elements do.

We have in TM case for a scattering diagram

$$F_\theta^{TM} = i\,k_0/\varepsilon_0 \sum_{m=0}^{M}\cos(m+1)\phi\,(i\,k_0/\varepsilon_0\sin\theta)^m \times$$

$$\sum_{n=1}^{N}\{p_{nm}^0\cos\theta[G'_n + (\bar{\kappa}^e - \sin^2\theta\bar{\zeta})G_n] + q_{nm}^0(G'_n + \bar{\kappa}^h G_n)\}$$

$$-\,i\,k_0/\varepsilon_0\sin\theta\sum_{n=1}^{N} r_n^0(G'_n + \bar{\kappa}^h G_n)\ ,$$

$$F_\phi^{TM} = -i\,k_0/\varepsilon_0 \sum_{m=0}^{M}\sin(m+1)\phi\,(i\,k_0/\varepsilon_0\sin\theta)^m \times \sum_{n=1}^{N}\{p_{nm}^0(G'_n + \bar{\kappa}^e G_n)$$

$$+\,q_{nm}^0\cos\theta[G'_n + (\bar{\kappa}^h - \sin^2\theta\bar{\zeta})G_n]\}\ ,$$

where spectral functions with an over-lines are

$$\bar{\kappa}^e = \frac{i\cos\theta - \sqrt{\sin^2\theta - \varepsilon_1/\varepsilon_0}}{i\cos\theta + \sqrt{\sin^2\theta - \varepsilon_1/\varepsilon_0}}\ ,\qquad \bar{\kappa}^h = \frac{i\varepsilon_1\cos\theta - \varepsilon_0\sqrt{\sin^2\theta - \varepsilon_1/\varepsilon_0}}{i\varepsilon_1\cos\theta + \varepsilon_0\sqrt{\sin^2\theta - \varepsilon_1/\varepsilon_0}},$$

$$\bar{\zeta} = \frac{2(\varepsilon_1 - \varepsilon_0)}{(i\cos\theta + \sqrt{\sin^2\theta - \varepsilon_1/\varepsilon_0})\cdot(i\varepsilon_1\cos\theta + \varepsilon_0\sqrt{\sin^2\theta - \varepsilon_1/\varepsilon_0})}\ ,$$

$$G'_n = \exp\{ik_0 w_n\cos\theta\}.$$

Similarly, for TE case we have

$$F_{\phi}^{TE} = i\,k_0/\varepsilon_0 \sum_{m=0}^{M} \cos(m+1)\phi\,(i\,k_0/\varepsilon_0 \sin\theta)^m \sum_{n=1}^{N} \{p_{nm}^0 (G_n' + \bar{\kappa}^e G_n)$$
$$- q_{nm}^0 \cos\theta [G'_n + (\bar{\kappa}^h - \sin^2\theta\bar{\zeta}) G_n]\}$$
$$+ i\,k_0/\varepsilon_0 \sin\theta \sum_{n=1}^{N} r_n^0 (G'_n + \bar{\kappa}^e G_n)\,,$$
$$F_{\theta}^{TE} = i\,k_0/\varepsilon_0 \sum_{m=0}^{M} \sin(m+1)\phi\,(i\,k_0/\varepsilon_0 \sin\theta)^m \times$$
$$\sum_{n=1}^{N} \{p_{nm}^0 \cos\theta [G_n' + (\bar{\kappa}^e - \sin^2\theta\bar{\zeta}) G_n] - q_{nm}^0 (G'_n + \bar{\kappa}^h G_n)\}\,.$$

Here the same designations as for TM case are used.

In such a way, the Green tensor elements in a far zone do not contain any Sommerfeld integrals, so diagram components do. Thus, once unknown pole coefficients are determined, to calculate scattering characteristics it is sufficient to calculate just a combination of elementary functions.

2. MODEL II: SUBSURFACE DEFECT

We begin from the BVSP statement, keeping designations of paragraph 1. Let in the lower half-space D_1 there exists an axi-symmetrical cladding D_i (the void will be a special case) having a smooth surface ∂D, which symmetry axis coincides with an external normal direction to interface Ξ, see Fig. 1. Then introduce into consideration the Cartesian system, choosing its origin at the point $O = Oz \bigcap \Xi$ while Oz axis to be directed into D_0 down the symmetry axis (see Fig. 1). Statement of the BVSP here has a form

$$\nabla \times \mathbf{H}_t = ik\varepsilon_t \mathbf{E}_t; \quad \nabla \times \mathbf{E}_t = -ik\mu_t \mathbf{H}_t \quad \text{in } D_t, \quad t = 0,1,i\,, \tag{2.1a}$$

$$\begin{aligned} \mathbf{n}_p \times \left(\mathbf{E}_i(p) - \mathbf{E}_1(p)\right) &= \mathbf{n}_p \times \mathbf{E}_1^0(p), \\ \mathbf{n}_p \times \left(\mathbf{H}_i(p) - \mathbf{H}_1(p)\right) &= \mathbf{n}_p \times \mathbf{H}_1^0(p), \end{aligned} \quad p \in \partial D\,, \tag{2.1b}$$

$$\begin{aligned} &\mathbf{e}_z \times \left(\mathbf{E}_0(p) - \mathbf{E}_1(p)\right) = 0, \\ &\mathbf{e}_z \times \left(\mathbf{H}_0(p) - \mathbf{H}_1(p)\right) = 0, \end{aligned} \quad p \in \Xi, \tag{2.1c}$$

radiation/attenuation conditions at infinity ($z \neq 0$). (2.1d)

Here $\{\mathbf{E}_i, \mathbf{H}_i\}$ is a total field inside a cladding; $\{\mathbf{E}_t, \mathbf{H}_t\}$ $(t = 0,1)$ is a scattered field in D_0, D_1 and $\left\{\mathbf{E}_1^0, \mathbf{H}_1^0\right\}$ is a field of the refracted plane wave in D_1. As in the particle case (part 1), we construct the approximate solution to BVSP (2.1) on the base MDS [3]. When constructing, we shall detail only points differing from the particle case.

For a representation of the field in D_1 the multipole sources of electric (e) and magnetic (m) kinds have been used. Due to the fact the obstacle now is located in the lower half-space the Hertz vector components have a form

$$\begin{aligned} g_m^{e,h}(q, w_n) &= Y_m^1(q, w_n) - Y_m^1(q, -w_n) + \\ &\int_0^\infty J_m(\lambda\rho)\, \kappa^{e,h} \exp\{\eta_1(z + w_n)\}\, \lambda^{1+m} d\lambda\,, \end{aligned} \tag{2.2a}$$

$$f_m(q, w_n) = \int_0^\infty J_m(\lambda\rho)\, \varsigma \exp\{\eta_1(z + w_n)\}\, \lambda^{1+m} d\lambda\,,$$

$$Y_{nm}^1(q) = Y_m^1(q, w_n) = \frac{k_1}{i} h_m^{(2)}(k_1 R_{qw}) \times (k_1\, \rho / R_{qw})^m\,.$$

Here spectral functions $\kappa^{e,h}$ and ζ are

$$\begin{aligned} &\kappa^e = 2\mu_0 / (\mu_0\eta_1 + \mu_1\eta_0), \quad \kappa^h = 2\varepsilon_0 / (\varepsilon_0\eta_1 + \varepsilon_1\eta_0), \\ &\zeta = 2(\mu_1\varepsilon_1 - \mu_0\varepsilon_0) / \{(\varepsilon_0\eta_1 + \varepsilon_1\eta_0)(\mu_0\eta_1 + \mu_1\eta_0)\}. \end{aligned} \tag{2.2b}$$

When constructing the field representation inside the defect we base on those multipole sources which singularities lie at the infinity. In this case the defect assumes to be filled with any substance (not only with an air). By the analogy with a particle case we construct an approximate solution that would take into account not only an axial symmetry of a geometry but the polarization of an external excitation as well. So, approximate solution we need has a form (1.5), but substituting (1.2) to (2.2).

In TM case the field of refracted plane wave in the lower half-space has a form

$$\mathbf{E}_1^0 = (\mathbf{e}_x\, T_p \cos\theta_t + \mathbf{e}_z\, T_p \sin\gamma \sin\theta_t\,)\chi_1, \quad \mathbf{H}_1^0 = -\mathbf{e}_y\, T_p n_1\, \chi_1,$$
$$\chi_1 = \exp\{-ik_1(x\sin\gamma - z\cos\gamma)\}, \tag{2.3a}$$
$$\sin\theta_t = n_0 / n_1 \sin\gamma, \quad \cos\theta_t = \sqrt{\varepsilon_1 - \varepsilon_0 \sin^2\gamma}\,/\,n_1, \quad n_{0,1} = \sqrt{\varepsilon_{0,1}\mu_{0,1}},$$

where the refraction coefficient is [5]

$$T_P = \frac{2n_0\, n_1 \cos\gamma}{\varepsilon_1 \cos\gamma + n_0\sqrt{\varepsilon_1 - \varepsilon_0 \sin^2\gamma}}$$

(2.3b)

For the case of TE polarization, when $\mathbf{E}^0$ vector is normal to the incident plane, the refracted plane wave field is

$$\mathbf{E}_1^0 = \mathbf{e}_y\, \chi_1\, T_S,$$
$$\mathbf{H}_1^0 = \mathbf{e}_x\, \chi_1\, T_S \sqrt{\varepsilon_1 - \varepsilon_0 \sin^2\gamma} + \mathbf{e}_z\, \sin\gamma\, \chi_1\, T_S\, n_0, \tag{2.4a}$$

and the refraction coefficient has a form

$$T_S = \frac{2n_0 \cos\gamma}{n_0 \cos\gamma + \sqrt{\varepsilon_1 - \varepsilon_0 \sin^2\gamma}}\,. \tag{2.4b}$$

As a result, the developed approximate solution to BVSP (2.1) with multipole sources, constructed in a special way, has a following properties:

1) fits the Maxwell equations inside a defect and in both half-spaces;
2) fits the transmission condition for field tangential components at the interface Ξ automatically;
3) satisfies the infinity conditions.

Due to the completeness of the multipole system and the orthogonality property of the multipole system for TM and TE polarizations at an arbitrary axi-symmetrical surface the following result take place.

Theorem 2. Let $\{\mathbf{E}_1^0,\ \mathbf{H}_1^0\}$: (2.3)/(2.4) then there exists Y and such coefficients $\{p_\upsilon, q_\upsilon\}_{\upsilon=\upsilon_0}^{\mathrm{Y}}$ that the approximate solution converge uniformly to the exact solution of BVSP (2.1) while $\mathrm{Y} \Rightarrow \infty$ at any closed compact outside the scatterer.

Note, the numerical scheme used for the construction of an approximate solution is completely analogous to the case of particle, but substituting matrix elements (because of the different representation for fields) and a total (incident plus reflected) field with the refracted one.

Before turn to the diagram representation for the case of subsurface defect we need in expressions for fields in upper half-space (because only there the scattering diagram has any sense). These expressions follows from (1.5), where index t is supposed to be 0. Moreover, the expressions for the Green tensor components from (1.5) will not any longer concur with formulas (2.2). Now the Green tensor components come to be the follows

$$g_m^{e,h}(q, w_n) = \int_0^\infty J_m(\lambda\rho)\, \kappa^{e,h} \exp\{-\eta_0 z + \eta_1 w_n\}\, \lambda^{1+m} d\lambda\,,$$

$$f_m^{e,h}(q, w_n) = \int_0^\infty J_m(\lambda\rho)\, \zeta^{e,h} \exp\{-\eta_0 z + \eta_1 w_n\}\, \lambda^{1+m} d\lambda\,,$$

$$\sigma_0^e = g_0^h, \qquad \sigma_0^h = \varepsilon_0 / \varepsilon_1 \cdot g_0^h,$$
$$\zeta^e = \zeta, \qquad \zeta^h = \varepsilon_0 / \varepsilon_1 \cdot \zeta,$$

and also the expressions for spectral functions are the same as (2.2b).

As before, the asymptotics are used to treat Sommerfeld integrals. Then spherical components of scattering diagram will have a form for TM case as

$$F_\theta^{TM} = i\,k_0/\varepsilon_0 \cos\theta \sum_{m=0}^{M} \cos(m+1)\phi\,(i\,k_0/\varepsilon_0 \sin\theta)^m \times$$
$$\sum_{n=1}^{N} G'_n\,\{p_{nm}(\bar{\kappa}^e + \bar{\zeta}) + q_{nm}\bar{\kappa}^h\} \;-\; i\,k_0/\varepsilon_0 \sin\theta \sum_{n=1}^{N} r_n\,G'_n\,\bar{\kappa}^h\ ,$$
$$F_\phi^{TM} = i\,k_0/\varepsilon_0 \cos\theta \sum_{m=0}^{M} \sin(m+1)\phi\,(i\,k_0/\varepsilon_0 \sin\theta)^m \times \tag{2.5}$$
$$\sum_{n=1}^{N} G'_n\,\{p_{nm}\bar{\kappa}^e + q_{nm}(\bar{\kappa}^h + \bar{\zeta}\,\varepsilon_0/\varepsilon_1)\}\ ,$$

and for TE case

$$F_\theta^{TE} = i\,k_0/\varepsilon_0 \cos\theta \sum_{m=0}^{M} \sin(m+1)\phi\,(i\,k_0/\varepsilon_0 \sin\theta)^m \sum_{n=1}^{N} G'_n\,\{p_{nm}(\bar{\kappa}^e + \bar{\zeta}) - q_{nm}\bar{\kappa}^h\},$$
$$F_\phi^{TE} = i\,k_0/\varepsilon_0 \cos\theta \sum_{m=0}^{M} \cos(m+1)\phi\,(i\,k_0/\varepsilon_0 \sin\theta)^m \times \tag{2.6}$$
$$\sum_{n=1}^{N} G'_n\,\{p_{nm}\bar{\kappa}^e - q_{nm}(\bar{\kappa}^h + \bar{\zeta}\,\varepsilon_0/\varepsilon_1)\} + i\,k_0/\varepsilon_1 \sin\theta \sum_{n=1}^{N} r_n G'_n\,\bar{\kappa}^e.$$

The over-lined spectral function are

$$\bar{\kappa}^e = \frac{2\cos\theta}{\cos\theta + \xi}\ , \qquad \bar{\kappa}^h = \frac{2\varepsilon_0 \cos\theta}{\varepsilon_0 \cos\theta + \varepsilon_1 \xi}\ ,$$
$$\bar{\zeta} = \frac{2(\varepsilon_1 - \varepsilon_0)}{(\cos\theta + \xi)\cdot(\varepsilon_0 \cos\theta + \varepsilon_1 \xi)}\ ,$$
$$G'_n = \exp\{ik_0\xi\},\quad \xi = \sqrt{\varepsilon_1/\varepsilon_0 - \sin^2\theta}.$$

3. MODEL III: ADVANCED FRESNEL APPROXIMATION

In many engineering applications there is no need in elegant mathematical models; and one seems to be quite sufficient to have a model which keeps just basic features of scattering yet can not produce a high accuracy. In the paper [8] the Fresnel approach (FA) has been implemented for a simulation of light scattering from spherical particles on a substrate. Such an approximation was shown to allow to reach reasonable results even

for the particle diameter as big as a half wavelength of an exciting field. However, FA [8] ignores a tensor relationship between dipoles and vector potentials, while this relationship really takes a place for a strict approach (for instance, the horizontal dipole must generate a vertical component of the vector potential besides the horizontal one [3]).

We suggested instead the Advanced Fresnel Approach (AFA), which enables to keep a tensor relation between sources (either dipoles or multipoles) and the vector potential (the Hertz vector). This approach allows us to increase a simulation accuracy and is most useful for scattering from complex defects. Let's have a look at (1.2a)/(2.2a). FA [8] means that

$$g_m^{e,h}(q,w_n) = Y_m^0(q,w_n) \mp r_p Y_m^0(q,-w_n),$$
$$r_p = \frac{\sqrt{\varepsilon_1} - \sqrt{\varepsilon_0}}{\sqrt{\varepsilon_1} + \sqrt{\varepsilon_0}}. \tag{3.1}$$

As it can be seen see from (3.1), there is no need in computing Zommerfeld integrals, which is the most expensive procedure. The explicit physical formula (3.1) can be also obtain from the strict approach by setting a parameter λ to be zero in spectral functions $\kappa^{e,h}$, $\zeta^{e,h}$ (1.2b)/(2.2b) of integrands (the quasi-static approximation). We call as AFA barely the same approach but being implemented to the whole Green tensor $\vec{\vec{\mathbf{G}}}^{e,h}(M,P)$. Then we have for non-diagonal terms

$$f_m(q,w_n) = \zeta_0 Y_m^0(q,-w_n), \quad \zeta_0 = \frac{2i(\varepsilon_0 - \varepsilon_1)}{k(\sqrt{\varepsilon_0} + \sqrt{\varepsilon_1})^2 \sqrt{\varepsilon_1}}. \tag{3.2}$$

The formulae (3.1) and (3.2) together represent the approach which we call as Fresnel-2 approximation, while neglecting (3.2) (i.e. an existence of elements $f_m^{e,h}$), Fresnel-1 (being, in fact, just FA [8]) is pro. And neglecting the Fresnel coefficient r_p in (3.1), we obtain the Fresnel-0 approximation, the most rough of all three. For this model the half-space is taken into account only through the excitation field and scattering diagrams. The same, of coarse, is valid for the pit scattering analysis too.

So, AFA allows to represent the scattered field in a clear analytic form both for near and far zones. The computations demonstrated AFA enables to get a moderate accuracy and accelerate computing as much as 10-30 times.

4. NUMERICAL RESULTS AND DISCUSSION

The demonstrated in the present work results illustrate the opportunities of the MDS realization, enabling to analyze scattering from silicon wafer defects of various types. Here the calculation of unknown source amplitudes and scattering characteristics was being realized in a parallel for all the incident angles of the plane wave and both linear polarizations. The numerical results given correspond to the exciting wavelength as λ = 0.488 μm, so that the dimensionless wave parameter *ka* is completely determined by the particle diameter. Only spherical particles will be regarded. All the dependencies presented are the scattered intensities (dimension μm^2) at the incident plane (i.e. azimuth half-planes 0° and 180°)

$$I^{TM,TE}(\theta,\phi) = \left|F_\theta^{TM,TE}(\theta,\phi)\right|^2 + \left|F_\phi^{TM,TE}(\theta,\phi)\right|^2 .$$

versa the scattering angle θ. The particle is supposed to be located at the plane interface of a dielectrical substrate (a wafer) having the refractive index $n = 4.5 - 0.4i$ corresponding to the silicon.

The detail investigations of particles of different kinds have been carried out. The most important fact established as a result of experiments is that for small particles the scattered field intensity for TM polarized plane wave for an oblique incidence does not decrease as one believed earlier [7], but increases instead. Moreover, the intensity increases as in the specular direction, and in the backward one. The use of this fact by disposing collectors in a proper way allows to increase the resolving ability of surface scanners.

The basic scattering properties of particles on substrate taking place independently on the particle material can be summarized as following:

- for "big" particles the scattered intensity for TE polarization exceeds the intensity for TM case over the whole range of scattering angles (see Fig. 2);

- for "small" particles the scattered intensity for TM polarization exceeds the intensity for TE case almost everywhere (Fig. 2) except a narrow segment close to a normal to the interface.

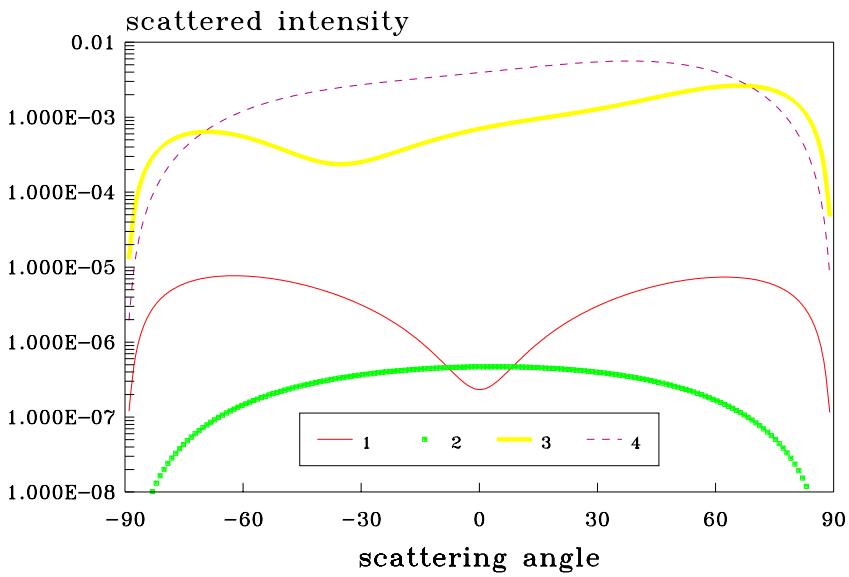

Figure 2. Scattering from a spherical PSL particle (the refractive index is 1.59). 'Small particle' (0.07 μm): 1, 2; and 0.20 μm: 3, 4. The wave incidence is –65°; TM polarization: 1, 3, TE case: 2, 4.

Now let's turn to analyzing of pit scattering properties. As it was been noticed previously, the problem how to distinguish particles upon a wafer interface from pits and subsurface defects comes to be more and more urgent last time. To analyze this problem we accomplished a numerical experiment, resulting in some characteristic features for defects of each type and enabling to distinguish particles and pits. Note, pits arise as a result of the crush of crystal organized particles [2], being just crystals built in the substrate. These pits have sizes from 0.07 μm to 0.2 μm, shaping as thetrahendrons with vertices α varying from 60° to 90°. Such defects are simulated as axi-symmetrical cones with smoothed tips and edges. The results of calculations for such cones are shown in

Figs 3, 4 the vertices 60° and 90°, aperture diameters 0.07 μm and 0.2 μm. Some typical features for all pits are:

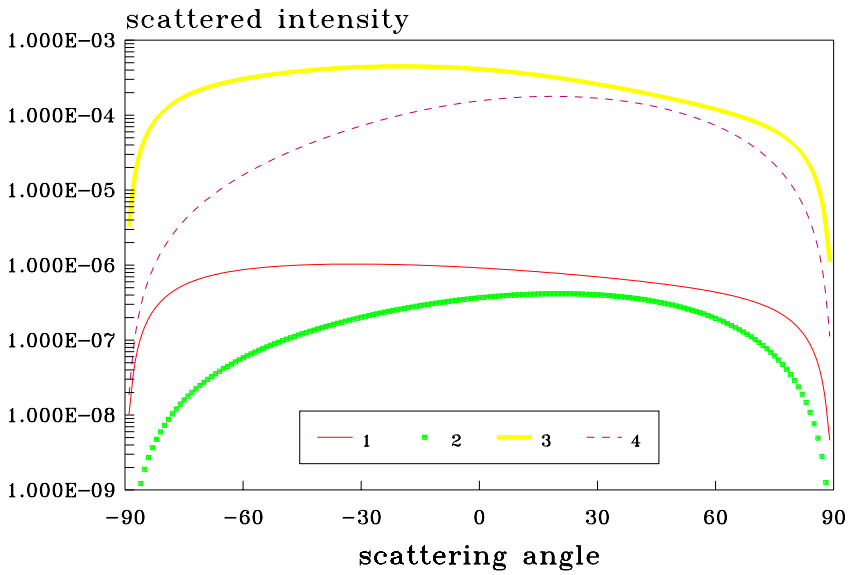

Figure 3. Scattering from a conical pit (the cone vertex angle is 60°), the base diameter is 0.07 μm (1,2) and 0.2 μm (3,4). Plane wave incidence is –65°; TM polarization: 1, 3, TE polarization: 2, 4.

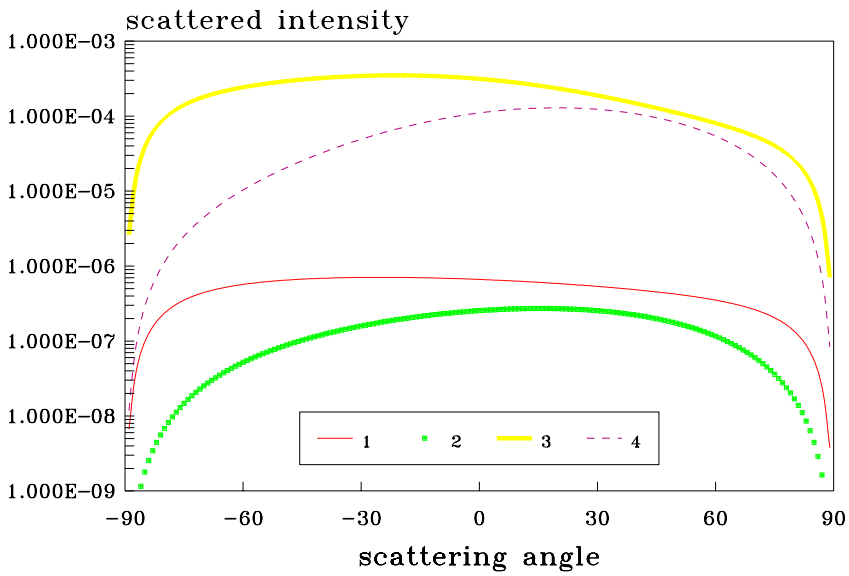

Figure 4. Scattering from a conical pit (the vertex angle is 90°). The markers have the same meaning as in Fig. 5.

- scattered intensity for TM polarization everywhere exceeds the intensity for TE case;
- for any pit the backward intensity in TM-case essentially exceeds the corresponding intensity for TE-case;
- at the range of scattering angles from 30° to 60° the difference between TM- and TE- cases is minimal.

Emphasize, these properties keep for pits of other geometries as well (for instance, conical pits of vertex 110°, and also for half-spherical pits). In Fig. 5 the scattering intensity for SiO_2 particle is shown (refractive index is 1.44) as compared with scattering from a pit (vertex angle 60°).

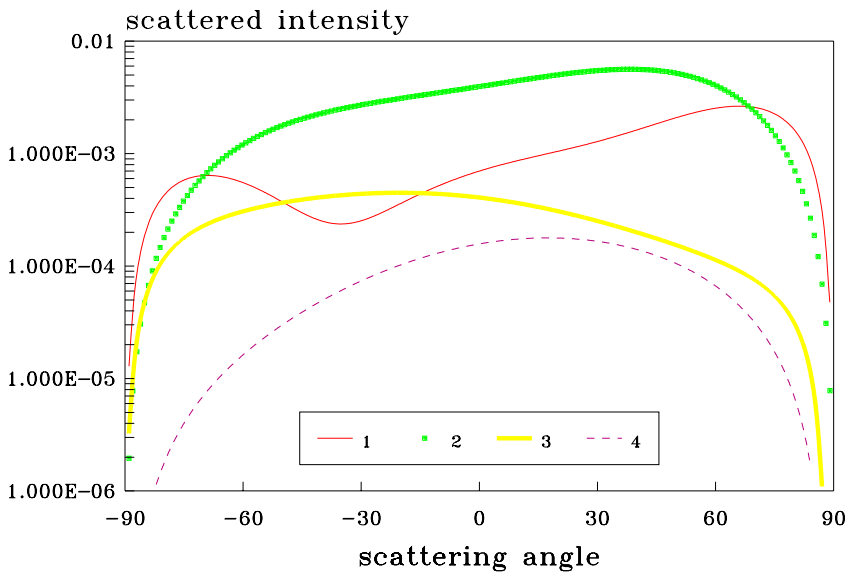

Figure 5. Results of scattering from a SiO_2 particle (1,2) as compared with scattering from a conical pit (3,4: the cone vertex angle is 60°). Plane wave incidence –65°, TM polarization.

In Figs 6, 7 the AFA is demonstrated as compared with the complete MDS model. The oblique (–65°) incident TM/TE plane wave and pits of different sizes and configurations are regarded. As it can be seen from Figs 6, 7, the AFA shows a pretty good agreement with MDS for quite big pit diameters.

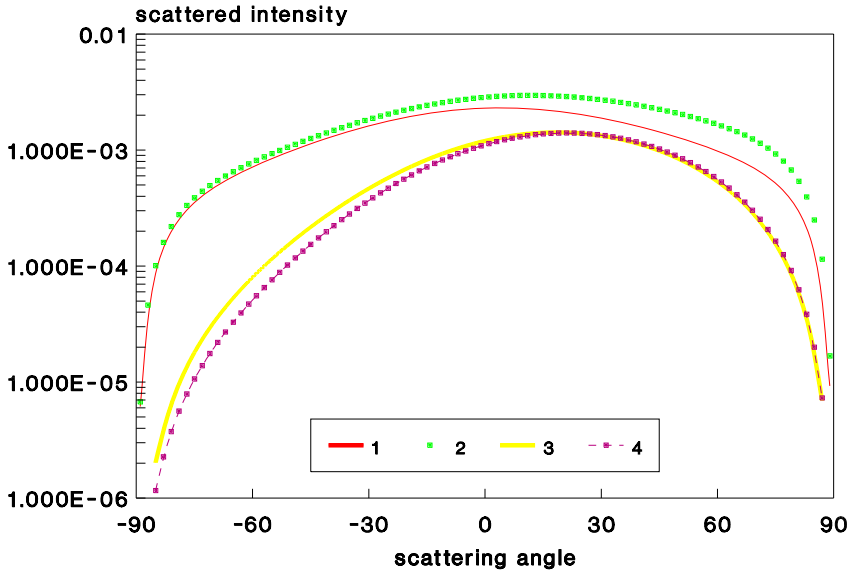

Figure. 6. Scattering from a conical pit. The cone vertex angle is 60°, the base diameter is 0.30 μm. Results from the complete model (1:TM, 3:TE) are compared with AFA, Fresnel-2 (2:TM, 4:TE). Plane wave incidence is –65°.

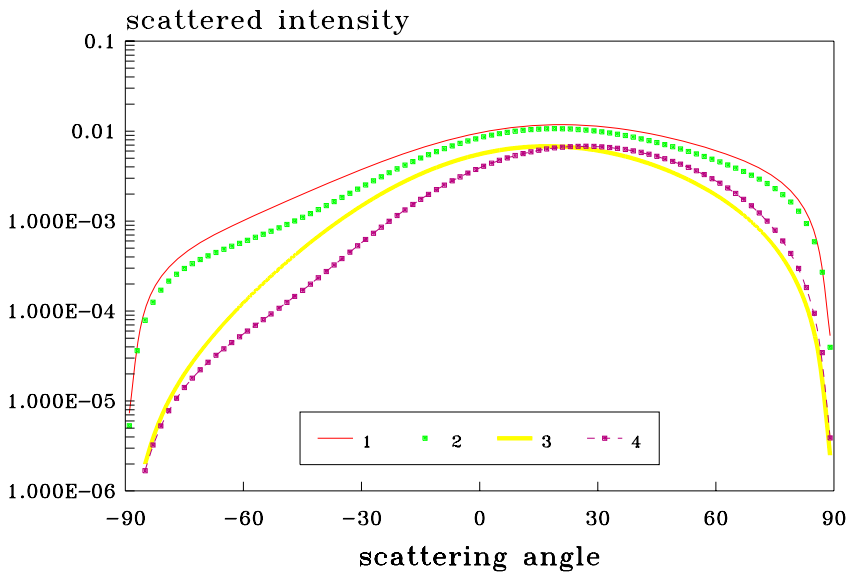

Figure 7. The same notation as in Fig.6 are used but the cone vertex angle is 100°, the base diameter is 0.488 μm.

In Figs 8, 9 there are some more illustrations of the AFA method for scattering from defects of different kinds. Fig. 8 corresponds to scattering from the Si sphere (D = 0.20 μm), the inclination of TM-polarized beam is –65°. Here curves 1, 2, 3 respond to MDS, Fresnel-1 and Fresnel 2, respectively. Fig. 9 corresponds to scattering from the pit (cone: vertex angle is 100°, D = 0.30 μm) when the TM-polarized beam incidents normally. We see in Figs 8,9 AFA produces an adequate results for both kinds of wafer defects, being quite good as compared with the explicit model (MDS).

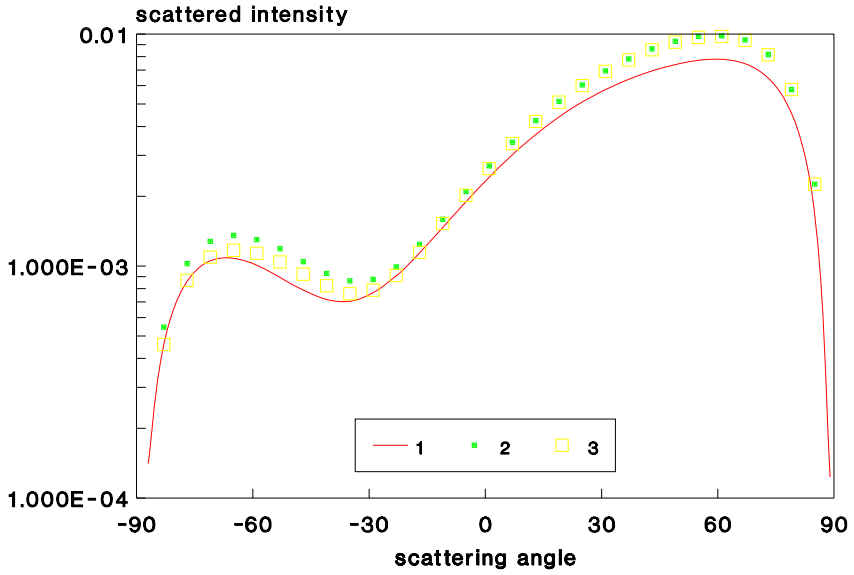

Figure 8. Scattering from a Si 0.2 μm sphere. The inclination of the TM-polarized beam is –65°. Curves 1, 2, 3 respond MDS, Fresnel-1, and Fresnel-2.

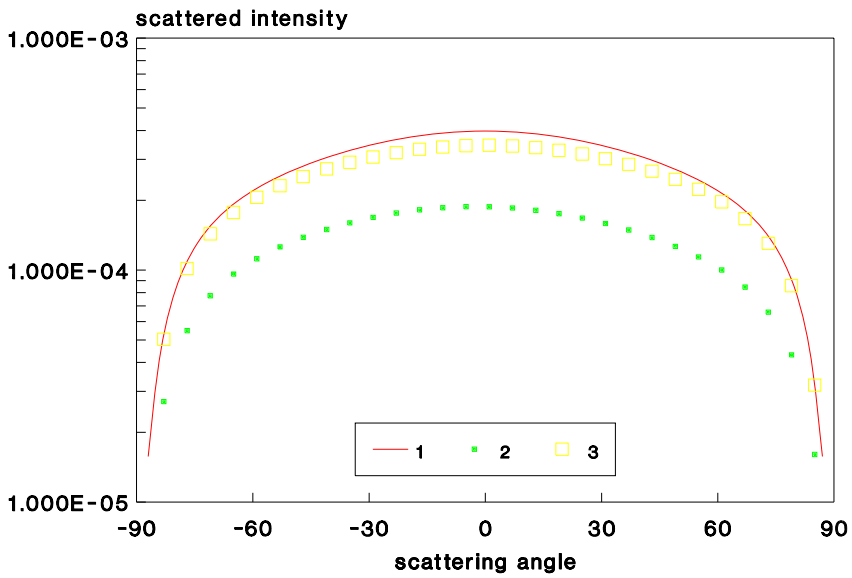

Figure 9. Scattering from a conical pit. The cone vertex angle is 60°, the base diameter is 0.30 μm. The inclination of the TM-polarized beam is –65°. Curves 1, 2, 3 respond MDS, Fresnel-1, and Fresnel-2.

Basing on the investigation fulfilled one may establish the conclusions.

1. Using the collector system of a surface scanner CR-80 [2] it is possible to distinguish a particle (any size, any material) from a pit (any diameter). Saying CR-80 we mean a system containing three cylindrical collectors being oriented orthogonally to the incident plane and centered with three different angles. Using the TM- and TE- polarized laser source and calculating the ratio of TE-scattered intensity to TM- one it is possible to distinguish pits from particles.

2. AFA appears to be justified when there is no need in a comprehensive analysis of scattering. Despite of its moderate accuracy AFA accelerates computing considerably and is adequate for engineering applications.

REFERENCES

[1] Huff H. et al. "Measurement of silicon particles by laser surface scanning and angle-resolved light scattering " //SEMATECH Meeting: Particle Counting / Microroughness Task Force. – Minneapolis, June 23-24, 1994.

[2] Fujino N. et al. Japanese J. of Appl. Phys., 1995. **12**.

[3] Eremin Yu. and Sveshnikov A., "Method of discrete sources in scattering problems (in Russian)". Moscow University Press, 1992.

[4] Yeremin Yu., Orlov N., and Sveshnikov A., J. of Commun. Technol. & Electronics, 1993. **38**(1).

[5] Born M. and Wolf E., "Principles of optics; electromagnetic theory of propagation, interference and diffraction of light". Oxford, NY: Pergamon Press, 1975.

[6] Felsen L. and Marcuvitz N., "Radiation and scattering of waves". NY: IEEE Press, 1994.

[7] Liu B., Chae S., Bae G. J. Electrochem. Soc., 1993. **140**(5).

[8] Johnson B., J. Optical Soc. Am.(A), 1996. **13**(2).